24th ABCM International Congress of Mechanical Engineering
December 3-8, 2017, Curitiba, PR, Brazil

COBEM-2017-0859
VELOCITY AND POSTURE SELECTION FOR TORQUE OPTIMIZATION IN MANIPULATORS WITH TWO-DIMENSIONAL FORCE REQUIREMENTS

Diego Gabriel Gomes Rosa
Marco Antonio Meggiolaro
Pontifícia Universidade Católica do Rio de Janeiro - R. Marquês de São Vicente 225, Gávea, Rio de Janeiro, RJ - Brazil - 22451-900
diegorosa@aluno.puc-rio.br; meggi@puc-rio.br

José Flávio Silveira Feiteira
Universidade Federal Fluminense - Av. dos Trabalhadores 420, Vila Sta. Cecília, Volta Redonda - RJ, Brazil - 27255-125
joseflavio@vm.uff.br

Abstract. *This work presents a methodology to perform a combined torque and time optimization for trajectories with particular force requirements. Usually, to reduce the time interval of a trajectory, elevated torques are required, an issue mainly when the mechanism needs to spend part of its energy to apply forces on its environment. In order to find a solution for this problem, an optimization method can be adopted. Here, the procedure is divided in two phases. First, a manipulator posture is chosen to minimize the total applied torques on the robot joints, performed by using a recently developed technique. Afterwards, from the selected posture, a set of possible joint velocities is simulated. The goal of this process is to find a threshold for the time trajectory from which the torque on the robot joints is not largely intensified. The dynamics based on a Lagrangian formulation of a two-link serial arm is applied for the mechanical modeling. By carrying out the analysis, it is possible to relate the robot posture, the velocity and the forces applied on the robot end-effector with the torque on the robot joints, to find an optimal trajectory.*

Keywords: *minimum time, optimal trajectory, torque minimization, velocity selection.*

Nomenclature:

B: Inertia matrix
C: Matrix of Coriolis and centripetal terms
g: Gravitational acceleration
h: Forces on the end effector
J: Jacobian matrix
PI: Performance Index
q: Position on the joint space
t: Time of simulation
τ: Torque on the joint space

1. INTRODUCTION

Optimization is a field of engineering with extensive research subjects, as it is used to improve the quality of products and processes. In robotics, this methodology is used in diverse areas, such as in trajectory planning, motion control, development of dynamical models or optimal design of industrial and mobile robots (Mombaur, *et al.*, 2014).

A particular use of optimization techniques is in robots that require environment interaction. In this case, even though interesting solutions already exists, different and enhanced approaches can always be developed in order to improve specific robot parameters. On industrial robots, for instance, developments in computational vision and force control strategies are common solutions that promote the robot perception of its environment (Romanelli, 2011). For example, the use of force control can support the execution of high accurate movements. It is notable in assembly or general machining operations (Alici, 1999), even if related advances can also be found in collaborative and service robots (Ceccarelli, 2011).

In both cases, the expansion of these fields of study can be heightened if an optimization treatment is adopted in concomitance with a well established procedure. However, in some circumstances, the optimization is not only a tool to facilitate a process, but a necessary way to compensate intrinsic limitations of the process. Serial manipulators are an interesting example. These robots can be implemented in operations with force interaction, usually in industrial tasks.

However, they have limitations related to its typical low stiffness. Hence, if there are not negligible forces acting in the robot end effector and these forces act in multiple directions, as occurs in machining operations, some robot parameters should be adjusted (Zaeh and Roesch, 2014). One of these parameters, normally linked to the robot performance, is the total torque on the joints.

In order to minimize the total torque, diverse techniques can be adopted. In this work, the robot posture and the end effector velocity are optimized. In fact, a robot pose is naturally associated with the torques on the joint space. If a pose increases the moment of inertia of the structure, problems related to inaccuracies can be originated. However, to find an optimal posture to a robotic task is not enough.

If the robot posture can improve the rigidity and the accuracy of a planned task, the same task could be improved if the planned trajectory is accomplished in a minimal time. It means that the maximum workspace velocity should be used, as long as it does not influence the torque on the robot joints. To relate two or more different parameters, as done by Feddema (1996) is a challenge. Therefore, it consists in the main goal of this work: to develop a methodology that can attach minimal torque and minimal time in order to accomplish a general robotic task.

2. METHODOLOGY

This work deals with trajectory optimization of industrial robots. According to Ata (2007), numerous strategies can be used to achieve this objective. Exhaustive search, genetic algorithms, analytical optimization and kinematics and dynamical approaches are some ways to develop a functional procedure. Rosa and Feiteira (2017), based on the dynamics of a serial manipulator, developed a performance index to compute and minimize the joint torques, and proposed a surface evaluation for posture selection of robots with two-dimensional force requirements. This computational technique is adopted here.

The first step in the optimization process consists in finding the vector of torques on the robot joints. It can be expressed as a dynamical function of diverse parameters: the position vector on the joint space, the mass and length parameters of the robot, the gravitational and contact forces, the Jacobian and the gear reductions ratios of the actuators. Simplifying, it can be expressed in Eq. (1), adapted from Corke (2011). This equation is developed from the Lagrangian formulation for a n-link robotic arm without friction loses.

$$\boldsymbol{\tau} = \mathbf{B}(\boldsymbol{q})\ddot{\boldsymbol{q}} + \mathbf{C}(\boldsymbol{q},\dot{\boldsymbol{q}})\dot{\boldsymbol{q}} + \boldsymbol{g}(\boldsymbol{q}) + \mathbf{J}^{\mathbf{T}}(\boldsymbol{q})\boldsymbol{h} \tag{1}$$

The performance index, PI, is presented in Eq. (2), adapted from Rosa and Feiteira (2017). It consists of an integral of the computed torque during the time of the simulation. The inverse exponent is used as a strategy to relate the addition in the performance index as an addition in the capacity of accomplish an optimized trajectory with minimal torque requests.

$$PI = \left(\int_0^{t_f} \|\boldsymbol{\tau}(t)\|\, dt\right)^{-1} \tag{2}$$

By considering a particular movement, it is possible to select a posture that guarantees the minimal torque on the joints. Afterwards, the best obtained pose can be used in simulations with different end effector velocities. In this case, the direct dynamics is used to compute the torque as a function of the velocities. By admitting that an increasing on the velocity increases the total torque, but considering a threshold to this, it is possible to reduce the total time of a task execution without high loses in the optimization process. In this case, the torque comparisons are computed by the average of the absolute torque contribution of all robot joints.

3. SIMULATIONS

A two-link planar serial arm model is used to generate the simulation results. It is used as a simplification of a 6 DOF industrial robot, on which links 2 and 3 can be represented by the planar arm. In fact, these two links are the most force requested in general robotic operations with load requests. An ABB IRB 2400 robot was used as model to the simulations, to turn the simulations as similar to a real case operation as it is possible. Some robot parameters are shown in Tab. 1. The terms a_1 and a_2 [m] represent the lengths of the robot links. The mass of the links are m_{l1} and m_{l2} [Kg], the moment of inertia of the links are I_{l1} and I_{l2} [Kgm²], the mass of the motors are m_{m1} and m_{m2} [Kg], the moment of inertia of the motors are I_{m1} and I_{m2} [Kgm²], and the gear reduction ratios are k_1 and k_2 . The presented values are approximations from real robot parameters.

Table 1. Parameters used in the simulations

a_1	a_2	m_{l1}	m_{l2}	I_{l1}	I_{l2}	m_{m1}	m_{m2}	I_{m1}	I_{m2}	k_1	k_2
0.84	0.75	50	40	10	5	5	5	0.010	0.005	100	100

The optimization procedure is specific for each robot trajectory. Thus, the chosen movement to be used in the simulations was based in a real case machining operation, as made by Rosa, *et al.* (2017). The robot end effector is moved in a point-to-point trajectory based on a third order polynomial trajectory. The initial velocities were considered null and the end effector orientation was disregarded. The mass of links and motors were considered to be applied in the structure's midpoint.

A particular movement executed in this work is shown in Fig. 1. The robot end effector moves from point A to point B in x-axis direction. The travelled distance is fixed in 0.5 m. Initially, a force $F_x = 200\ N$ is considered to be applied on the robot tool, as it is usual in milling operations, for example. Another force, $F_y = 200\ N$, is also applied. It represents the effects of the spindle and the force sensor masses on the robot structure. The end effector linear velocity is initially set to 5 mm/s, value responsible for a simulation time of 10 seconds. The frequency of data processing is set to 50 Hz.

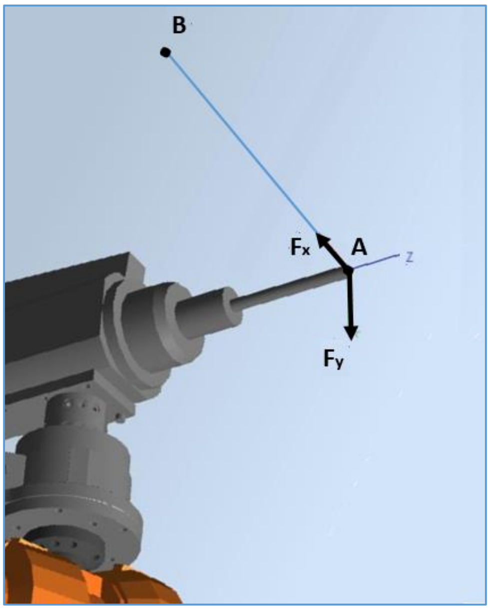

Figure 1. Trajectory and forces executed by the manipulator

3.1 Torque optimization based on joint positioning

In order to accomplish the main objective of this work, the first step to be executed is to find a region on which the robot posture minimizes the torques on the robot joints. As stated previously, if low torques are applied to the joints, the rigidity and, consequently, the accuracy of the robot are increased. Rosa and Feiteira (2017) used an algorithm that generates all possible initial configurations for a robot that executes a trajectory, as the one specified in Fig. 1. In this case, the ABB IRB 2400 robot workspace was set as the basis for the movement. Hence, the joint torques for the entire movement were computed for the cited configurations and a performance index was obtained, according to Eq. (2), from the obtained torque values.

Moreover, to facilitate the process of choosing an optimal position, an evaluation surface can be found with a set of performance indexes related to all initial joint positions. The higher indexes that do not coincide with singularities configurations are natural candidates for the optimization. Figure 2 shows a particular evaluation surface to the trajectory executed in this work. There, a high performance index region can be randomly selected from a path starting in the position 2.2 rad for the first joint and –0.985 rad for the second joint of the robot. When the robot direct dynamics is applied, the torques in Fig. 3(a) are found. In this case, the path has 10 seconds of duration.

It is necessary to note that the plotted surface is a function only of the joint positions. It means that, even though the torques consider instantaneous accelerations and velocities of the robot joints, this analysis is very particular and contrasts to the range of possible end effector velocities that the robot can assume. In fact, for a complete analysis, a different surface should be generated for each end effector velocity, by considering the robot speed range. Besides, in usual machining operations, for instance, this velocity is a system input. Thus, this method can be useful for specific tasks that need specific velocities or if only a few set of velocities needs to be analyzed.

Conversely, this theory of pose optimization can be extended, since the surfaces' shapes keep a constancy in a large portion of the robot speed range. Figure 3 shows four usual velocities and the surfaces related to them, for the trajectory here used. In this figure, it is possible to verify that the changings in the surface's shape are gradually happening as the velocity is increased. Therefore, there is a direct relation between joint torques and end effector velocities. However, the performance index is not able to denote physically what is happening.

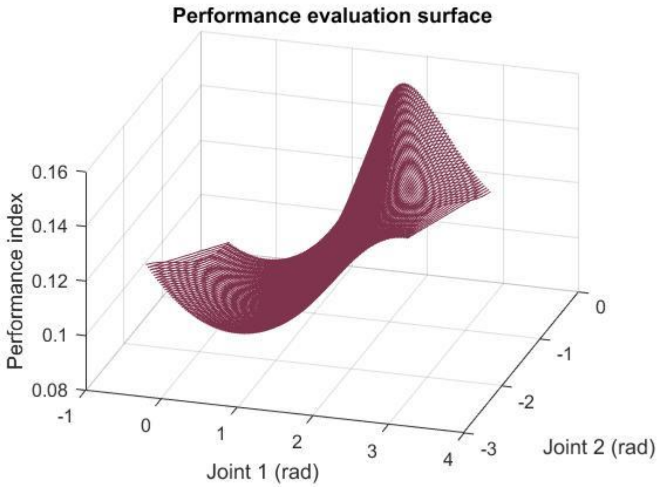

Figure 2. Evaluation surface for a two link planar arm

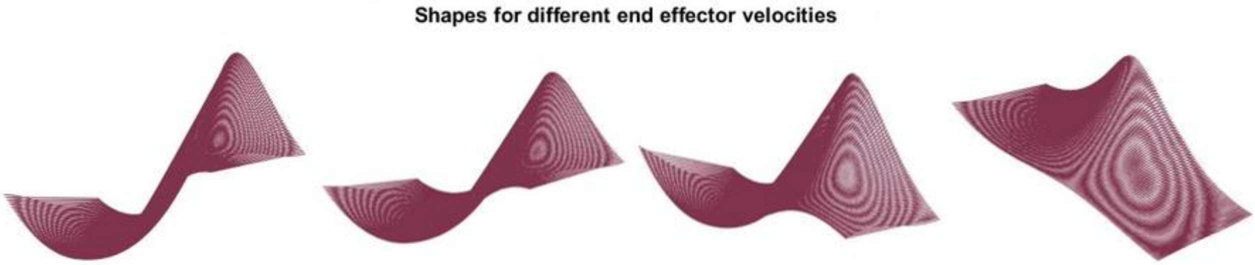

(a) (b) (c) (d)

Figure 3. Surface's shapes and end effector velocities: a) 5 mm/s, b) 10 mm/s, c) 20 mm/s, d) 50 mm/s

In fact, a more detailed analysis can be performed if the end effector velocity is examined with the robot poses. It has a theoretical and a practical importance. In industrial applications, a process need to be made with the accuracy guaranteed by the pose optimization and in a minor time as it is possible. The surface evaluation is a fast method, though a different strategy with a physical interpretation could collaborate to the optimization process, as follows.

3.2 Time optimization

The performance indexes and the evaluation surfaces demonstrated to be interesting tools for torque optimization of a general industrial robot. However, these methods are attached to the end effector velocity, as it is possible to observe in Fig. 3. Hence, another method is necessary to optimize the velocities and times related to real case robot applications.

In this way, the first estimated solutions can be based on methods and algorithms related to exhaustive search. Founded in this theory, it would be possible to simulate, as made previously, all possible end effector velocities to a set of possible initial positions. However, these are high-cost computational methods and in some cases not useful for industrial daily tasks. Thus, the previously obtained method to posture selection can be used as an initial guest to the current problem.

Figure 4 (a) shows a test with a velocity of 5 mm/s in the robot end effector for the previously studied trajectory. By simulating different velocities, as done in Fig. 3, new graphs can be generated to represent the torque curves for the same trajectory. Thus, if the end effector velocity is increased to 10 mm/s, larger torques appear in the joint space, as shown in Fig. 4 (b). In this case, the increasing in the joint torques is small, but present. However, only in Fig. 4 (c) and (d) the rising in the torques are better observable. In the last case, ten multiplies the original velocity and the torque in joint 2 is almost the double of the original one.

To compare the obtained results, a methodology needs to be adopted. Here, the average of torques, considering all robot joints together, is computed. The obtained values are shown in Tab. 2. In the first exposed case, the torque is related to forces of 200 N in two robotic axis directions. It is possible to observe the rising in the average torques, which reaches 368.5 Nm in a simulation with 50 mm/s velocity. However, by observing other velocities and torques, it is possible to note that it is not easy to find a relation between these values.

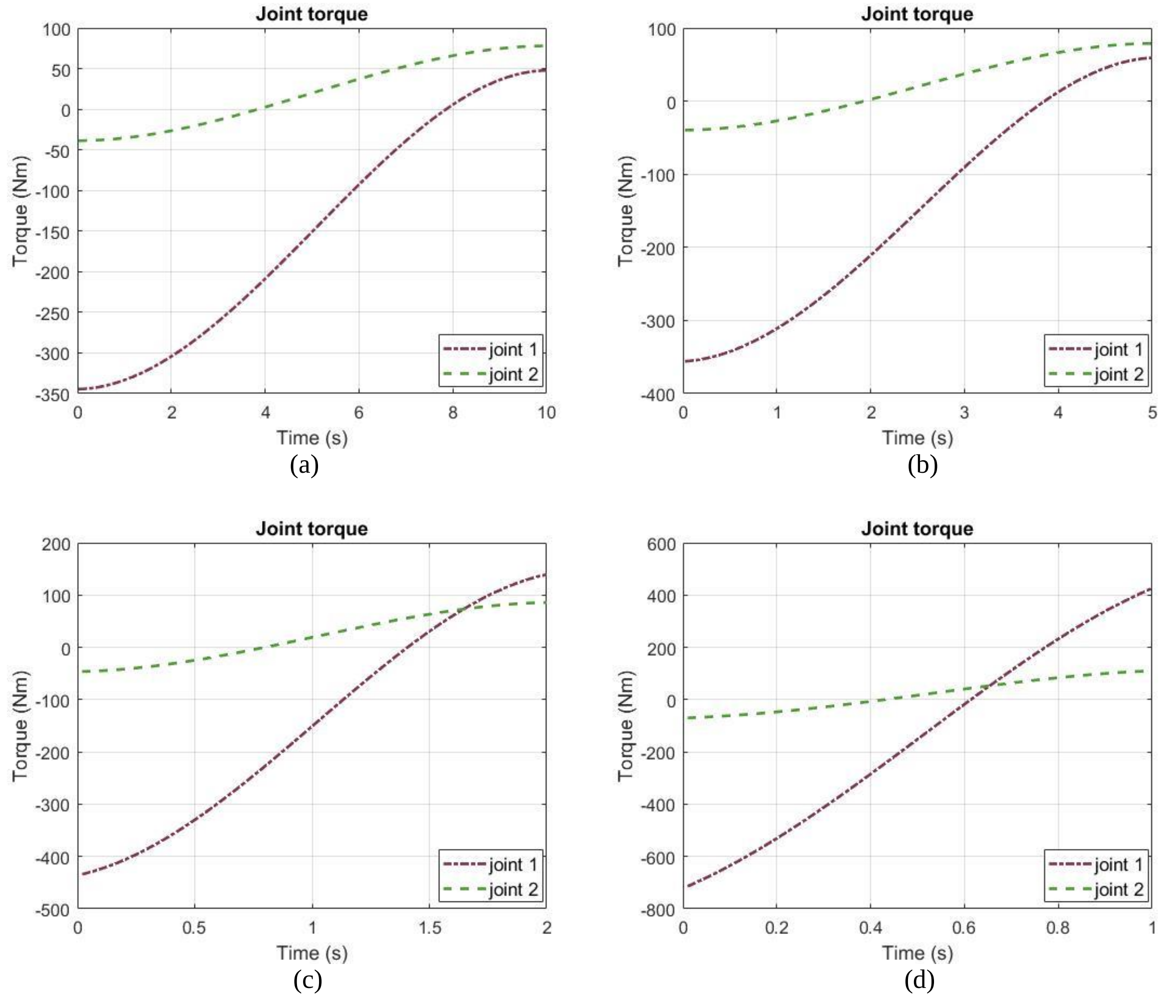

Figure 4. Simulations with variations on velocity of the end effector; a) original velocity; b) twice the original velocity; 5 times the original velocity; 10 times the original velocity

With a view to find a relation between torques and velocities, new simulations can be executed also for higher loads. If the force constraints are 1000 N and 200 N, for instance, new results are obtained. The velocities and torques related to this second case are also shown in Tab. 2. In this case, even small changes in the end effector velocity cause a considerable variation in the average joint torque. However, also in this case, for higher velocities, the changings in the joint torques are less expressive. If in the first case the torques are doubled, in this second case the maximum registered average torque is something about 28 % of the original.

Table 2 – Average torque and time influences for a general manipulator

	Velocity (m/s)	**5**	**10**	**20**	**25**	**50**
Average Torque (Nm)	**Case 1**	186.2	186.2	187.1	187.6	368.5
	Case 2	709.2	716.0	742.1	759.3	909.3

Moreover, this range of velocities, that demonstrated to have nonlinear relations with the joint torques, is only part of the range of a real robot. Hence, the full analysis have to consider the torque behavior to diverse end effector velocities. For a specific trajectory and force requirements, as made in the posture selection, a graph can be obtained in the simulation process. Figure 5 shows the curve for the end effector velocity as a function of different average torques in robot joints. As it is possible to observe, the average torque is practically linear in low velocities. It is expected, as the low velocities are normally related to low accelerations and the executed trajectory can be simplified as a quasi-static movement. In this case, the forces in the robot end effector are 200 N in two directions and the velocity of approximately 26 mm/s can be used as a threshold to the robot programming.

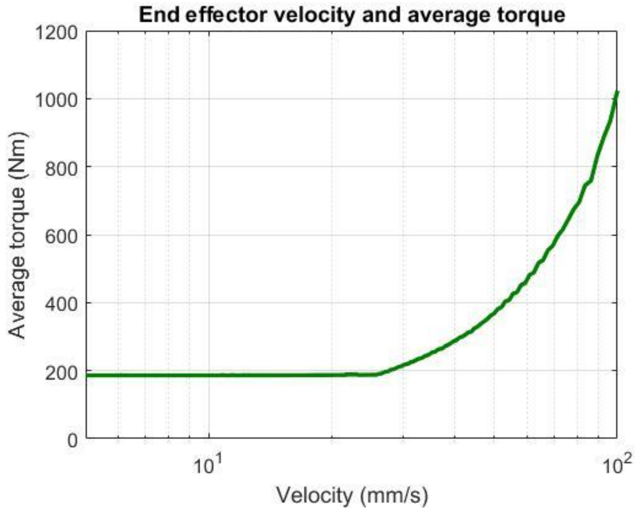

Figure 5. Relation between torque and velocity for low force requirements

Figure 6 can be similarly analyzed. Though, in this case, the simulated forces are 1000 N in x-axis direction and 200 N in y-axis direction. The linear region that appeared in Fig. 5 practically do not exists in Fig. 6. The maximum average torque in this figure is also higher. The velocity starts to make influence in velocities near 12 mm/s, that can be considered a threshold to avoid torque increasing for this specific trajectory and forces.

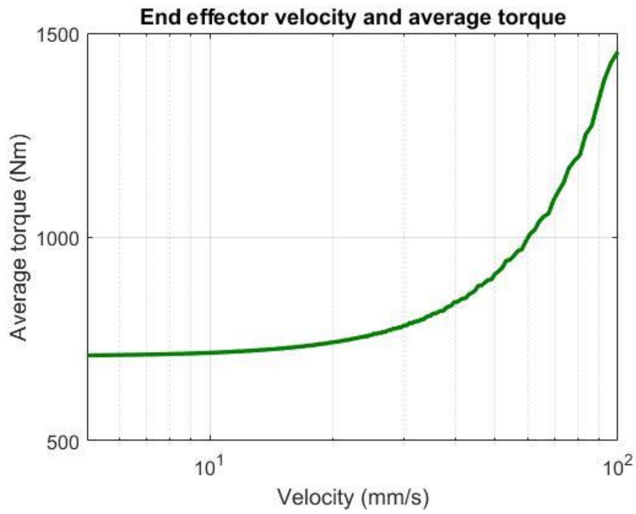

Figure 6. Relation between torque and velocity for high force requirements

By analyzing Fig. 5 and 6, and by considering that the horizontal axis is expressed as a logarithmic function, it is possible to infer that the torques and velocities have a quadratic relation. In fact, according to Eq. (1), $\dot{\boldsymbol{q}}$ and $\mathbf{C}(\boldsymbol{q}, \dot{\boldsymbol{q}})$ are the only contributions of the joint velocities in the torque vector. Since the velocity is computed as the first derivative of the third order polynomial that describes the robot trajectory, the torque function have to copy its quadratic behavior in some way. The contributions of $\mathbf{C}$ and $\boldsymbol{h}$ are also important and make influence on the difference of torques between the two studied cases.

Even if theoretical or numerical approaches are adopted, this review is significant when dealing with the manipulators' use in the industry. It is known that high velocities demand high dynamical requests and these velocities should always be avoided, especially in operations with robot interaction. However, on purpose of maintain a high production rate, the time to finish a task should always be reduced. Then, the analysis made in this work, by considering the velocities thresholds presented in Fig. 5 and 6, is a good solution for this problem.

Consequently, the union of the theory of time optimization with the previously presented theory of posture optimization, even they appear to dissent in their objectives and methodologies, can be useful in a large number of robotic applications. Furthermore, these techniques are easy to implement and do not requires high computational costs. Thus, they can be used inside the robot controller or in an external computer, in order to prevent loses in any industrial task.

For instance, suppose that a robot have to be used to drill an aircraft fuselage guaranteeing low torques on its joints and in a minimal time. Suppose also that the robot has a spindle as its tool and the spindle rotation can be used to reduce or increase the robot advance. If the robot is in the situation of Fig. 5 and a 10 mm/s velocity is adopted in an optimal posture, the task is accomplished. However, if the spindle velocity is controlled in order to double the robot advance (to 20 mm/s), the manipulator will spend a half of time to finish its task. In this example, the advance can be set to a value of 26 mm/s, always in order to minimize the total operation time. Thus, it shows the advantages of use optimization strategies and the importance of continuously improve the optimization techniques.

3.3 Summarization

As a form to simplify the use of the technique described, the diagram in Fig. 7 can be adopted. It is an intuitive manner to reproduce the steps for torque and time optimization. As it is possible to observe, the first step is the trajectory definition. It is the basis of both optimization processes. Later, the forces and moments in the robot end effector have to be estimated, in purpose of the computation of the robot kinematics and dynamics. The computed torques are then used in the performance index and the evaluation surface generation. With these tools, it is possible to select a posture that can minimize the joint torques while it avoid robot singularities. In the end, by using these torques in the robot trajectory, an average torque can be computed and compared to the possible end effector velocities. In this process, a threshold for the velocities can be found and this value guarantees the minimal time for a task accomplishing.

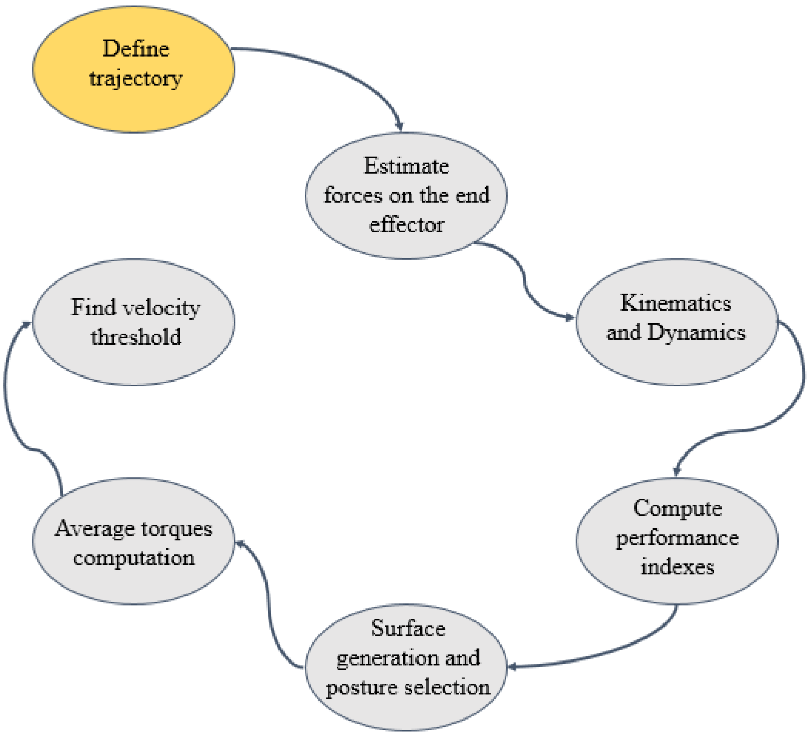

Figure 7. Step by step algorithm diagram

4. CONCLUSIONS

In this work, a detailed analysis of posture and velocity effects on joint torques of serial robots was conducted, based on simulations of a simplified robot model and its dynamical equations. By assuming the robot rigidity as a function of its configuration, it was possible to explore the pose selection of a robot that interacts with its environment and in a dynamical approach.

From the selected posture, that guarantees minimal torques in the robot joints, a second optimization was conducted. Now, to optimize the time interval necessary to accomplish a general task. In this case, a threshold is obtained from a set of possible velocities that the robot end effector can assume. This threshold have to guarantee a minimal time of operation and it cannot affects the torque on the joints. Thus, one optimization solution does not affects the other one. This process is very interesting, as it can be used directly in industrial fields and in experimental works.

It is important to observe that the process and figures were generated for a two link planar arm with force requirements in two directions. However, the method here presented can be generalized for robot with more than 2 DOFs and other forces or moments applied in its end effector.

5. REFERENCES

Alici, G., 1999. Systematic Approach to Develop a Force Control System for Robotic Drilling. *Industrial Robot: An International Journal*. Vol. 26, No. 5, p. 389 – 397. DOI /10.1108/01439919910284019.

Ata, A.A., 2007. Optimal Trajectory Planning Of Manipulators: A Review. *Journal of Engineering Science and Technology*. Vol. 2, No. 1, p. 32–54.

Ceccarelli, M., 2011. Problems and Issues for Service Robots in New Applications. *Int J Soc Robot*, Vol. 3, p. 299–312. DOI 10.1007/s12369-011-0097-8.

Corke, P., 2011. *Robotics, Vision and Control – Fundamentals Algorithms in MATLAB®*. STAR, Berlin and Heidelberg.

Feddema, J.T., 1996. Kinematically Optimal Robot Placement for Minimum Time Coordinated Motion, *SPIE*. Vol. 2596, p. 22–31.

Mombaur, K., Koch, K. H. and Felis, M., 2014. Model-based Optimization for Robotics. *The Robotics Society of Japan Journal*, Vol. 32, No. 6, p. 492–498.

Romanelli, F., 2011. Advanced Methods for Robot-Environment Interaction towards an Industrial Robot Aware of Its Volume. *Journal of Robotics*. DOI 10.1155/2011/389158.

Rosa, D. G. G. and Feiteira, J. F. S, 2017. An Algorithm to Improve the Ridigity on the Motion Planning of a Robotic Mechanism. In *Proceedings of XVII International Symposium on Dynamic Problems of Mechanics – DINAME 2017*. São Sebastião, Brazil.

Rosa, D. G. G., Feiteira, J. F. S., Lopes, A. M. and Abreu, P. A. F., 2017. Analysis and Implementation of a Force Control Strategy for Drilling Operations with an Industrial Robot. *J Braz. Soc. Mech. Sci. Eng*. DOI 10.1007/s40430-017-0913-7.

Zaeh, M. F. and Roesch, O., 2014. Improvement of the Machining Accuracy of Milling Robots, *Production Engineering Research and Development*. Vol. 8, p. 737–744.

6. RESPONSIBILITY NOTICE

The authors are the only responsible for the printed material included in this paper.